

High-Precision Electroweak SUSY Production Cross Sections at e^+e^- Colliders

S. Heinemeyer*

Instituto de Física Teórica (UAM/CSIC), Universidad Autónoma de Madrid, Cantoblanco, 28049, Madrid, Spain

Campus of International Excellence UAM+CSIC, Cantoblanco, 28049, Madrid, Spain

Instituto de Física de Cantabria (CSIC-UC), 39005, Santander, Spain

E-mail: Sven.Heinemeyer@cern.ch

C. Schappacher

Institut für Theoretische Physik, Karlsruhe Institute of Technology, 76128, Karlsruhe, Germany (former address)

E-mail: schappacher@kabelbw.de

For the search for electroweak (EW) particles in the Minimal Supersymmetric Standard Model (MSSM) as well as for future precision analyses of these particles an accurate knowledge of their production and decay properties is mandatory. We evaluate the cross sections for the chargino, neutralino and slepton production at e^+e^- colliders in the MSSM with complex parameters (cMSSM). The evaluation is based on a full one-loop calculation of all possible production channels including soft and hard photon radiation. The dependence of the cross sections on the relevant cMSSM parameters is analyzed numerically. We find sizable contributions to many production cross sections. They amount to roughly 15% of the tree-level results but can go up to 40% or higher in extreme cases. Also the dependence on complex parameters of the one-loop corrections for many production channels was found non-negligible. The full one-loop contributions are thus crucial for physics analyses at a future linear e^+e^- collider such as the ILC or CLIC.

Loops and Legs in Quantum Field Theory (LL2018)

29 April 2018 - 04 May 2018

St. Goar, Germany

*Speaker.

1. Introduction

One of the important tasks at the LHC is to search for physics beyond the Standard Model (SM), where the Minimal Supersymmetric Standard Model (MSSM) [1] is one of the leading candidates. Supersymmetry (SUSY) predicts two scalar partners for all SM fermions as well as fermionic partners to all SM bosons. Contrary to the case of the SM, in the MSSM two Higgs doublets are required. This results in five physical Higgs bosons instead of the single Higgs boson in the SM. These are the light and heavy \mathcal{CP} -even Higgs bosons, h and H , the \mathcal{CP} -odd Higgs boson, A , and the charged Higgs bosons, H^\pm . The neutral SUSY partners of the (neutral) Higgs and electroweak gauge bosons are the four neutralinos, $\tilde{\chi}_{1,2,3,4}^0$. The corresponding charged SUSY partners are the charginos, $\tilde{\chi}_{1,2}^\pm$. The SUSY partner of the charged leptons are the $\tilde{e}_s, \tilde{\mu}_s, \tilde{\tau}_s$ ($s = 1, 2$), the ones of the neutrinos are the $\tilde{\nu}_e, \tilde{\nu}_\mu, \tilde{\nu}_\tau$.

If SUSY is realized in nature and the scalar quarks and/or the gluino are in the kinematic reach of the (HL-)LHC, it is expected that these strongly interacting particles are eventually produced and studied. On the other hand, SUSY particles that interact only via the electroweak force, i.e., the charginos, neutralinos, and scalar leptons, have a much smaller production cross section at the LHC. Correspondingly, the LHC discovery potential as well as the current experimental bounds are substantially weaker [2, 3]. At a (future) e^+e^- collider charginos, neutralinos and sleptons, depending on their masses and the available center-of-mass energy, could be produced and analyzed in detail [4, 5]. Corresponding studies can be found for the ILC in Refs. [6, 7] and for CLIC in Refs. [7, 8]. (Results on the combination of LHC and ILC results can be found in Ref. [9].) Such precision studies will be crucial to determine their nature and the underlying SUSY parameters.

In order to yield a sufficient accuracy, one-loop corrections to the various production and decay modes have to be considered. Full one-loop calculations in the cMSSM of (heavy) scalar tau decays was evaluated in Ref. [10], where the calculation can easily be taken over to other slepton decays. Similarly, full one-loop calculations for various chargino/neutralino decays in the cMSSM have been presented in Ref. [11]. Sleptons can also be produced in SUSY cascade decays, where full one-loop evaluations in the cMSSM exist for the corresponding decays of Higgs bosons [12]. Similarly, the one-loop corrections for chargino/neutralino production from the decay of Higgs bosons (at the LHC or ILC/CLIC) can be found in Ref. [13]. Here we review the predictions for chargino, neutralino and slepton production at e^+e^- colliders [14, 15] (see also Ref. [16]), i.e. the channels (with $\tilde{e}_{gs} = \{\tilde{e}_s, \tilde{\mu}_s, \tilde{\tau}_s\}$, $\tilde{\nu}_g = \{\tilde{\nu}_e, \tilde{\nu}_\mu, \tilde{\nu}_\tau\}$, generation index g and slepton index s)

$$\sigma(e^+e^- \rightarrow \tilde{\chi}_c^\pm \tilde{\chi}_{c'}^\mp) \quad c, c' = 1, 2, \quad \sigma(e^+e^- \rightarrow \tilde{\chi}_n^0 \tilde{\chi}_{n'}^0) \quad n, n' = 1, 2, 3, 4, \quad (1.1)$$

$$\sigma(e^+e^- \rightarrow \tilde{e}_{gs}^\pm \tilde{e}_{g's'}^\mp) \quad s, s' = 1, 2, \quad \sigma(e^+e^- \rightarrow \tilde{\nu}_g \tilde{\nu}_g^*) \quad g = 1, 2, 3. \quad (1.2)$$

2. Calculation of diagrams

In this section we review some details regarding the renormalization procedure and the calculation of the tree-level and higher-order corrections to the production of charginos, neutralinos and sleptons in e^+e^- collisions. The diagrams and corresponding amplitudes have been obtained with `FeynArts` (version 3.9) [17], using our MSSM model file (including the MSSM counterterms) of Ref. [18]. The further evaluation has been performed with `FormCalc` (version 9.5) and `LoopTools` (version 2.14) [19].

The cross sections (1.1) - (1.2) are calculated at the one-loop level, including soft, hard and collinear QED radiation. This requires the simultaneous renormalization of the gauge-boson sector, the fermion/sfermion sector as well as the chargino/neutralino sector of the cMSSM, based on Refs. [18, 20]. All the relevant details can be found in Refs. [14, 15]. The renormalization scheme employed is the same one as for the decay of sleptons [10] or charginos/neutralinos [11]. Consequently, the predictions for the production and decay can be used together in a consistent manner. More details and the application to Higgs-boson and SUSY particle decays can be found in Refs. [10–13, 18, 21–23]. Similarly, the application to Higgs-boson production cross sections at e^+e^- colliders are given in Refs. [24, 25].

Sample diagrams for the process $e^+e^- \rightarrow \tilde{e}_{gs}^\pm \tilde{e}_{gs'}^\mp$ and $e^+e^- \rightarrow \tilde{\nu}_g \tilde{\nu}_g^*$ are shown in Fig. 1. Diagrams for chargino/neutralino production can be found in Ref. [14]. Not shown in Fig. 1 are the diagrams for real (hard and soft) photon radiation. We have neglected all electron–Higgs couplings and terms proportional to the electron mass whenever this is safe, i.e. except when the electron mass appears in negative powers or in loop integrals. We have verified numerically that these contributions are indeed totally negligible. Moreover, in general, in Fig. 1 we have omitted diagrams with self-energy type corrections of external (on-shell) particles. While the contributions from the real parts of the loop functions are taken into account via the renormalization constants defined by OS renormalization conditions, the contributions coming from the imaginary part of the loop functions can result in an additional (real) correction if multiplied by complex parameters. In the analytical and numerical evaluation, these diagrams have been taken into account via the prescription described in Ref. [18].

As regularization scheme for the UV divergences we have used constrained differential renormalization [26], which has been shown to be equivalent to dimensional reduction [27, 28] at the one-loop level [19]. Thus the employed regularization scheme preserves SUSY [29, 30] and guarantees that the SUSY relations are kept intact. All UV divergences cancel in the final result. For a discussion on soft photon emission and corresponding problems with the phase space integration, see Refs. [14, 15].

3. Numerical analysis

Here we review two examples for the numerical analysis of chargino/neutralino and slepton production at e^+e^- colliders in the cMSSM as presented in Refs. [14, 15]. In the figures below we show the cross sections at the tree level (“tree”) and at the full one-loop level (“full”), which is the cross section including *all* one-loop corrections. All results shown use the CCN[1] renormalization scheme [18] (i.e. OS conditions for the two charginos and the lightest neutralino).

3.1 The processes $e^+e^- \rightarrow \tilde{\chi}_c^\pm \tilde{\chi}_{c'}^\mp$ and $e^+e^- \rightarrow \tilde{\chi}_n^0 \tilde{\chi}_{n'}^0$

The SUSY parameters for the evaluation of these production cross sections are chosen according to the scenario S1, shown in Tab. 1.

As an example for chargino/neutralino production the process $e^+e^- \rightarrow \tilde{\chi}_1^+ \tilde{\chi}_1^-$ is shown in Fig. 2. In the analysis of the production cross section as a function of \sqrt{s} (upper left plot) we find the expected behavior: a strong rise close to the production threshold, followed by a decrease with increasing \sqrt{s} . Away from the production threshold, loop corrections of $\sim -8\%$ at $\sqrt{s} =$

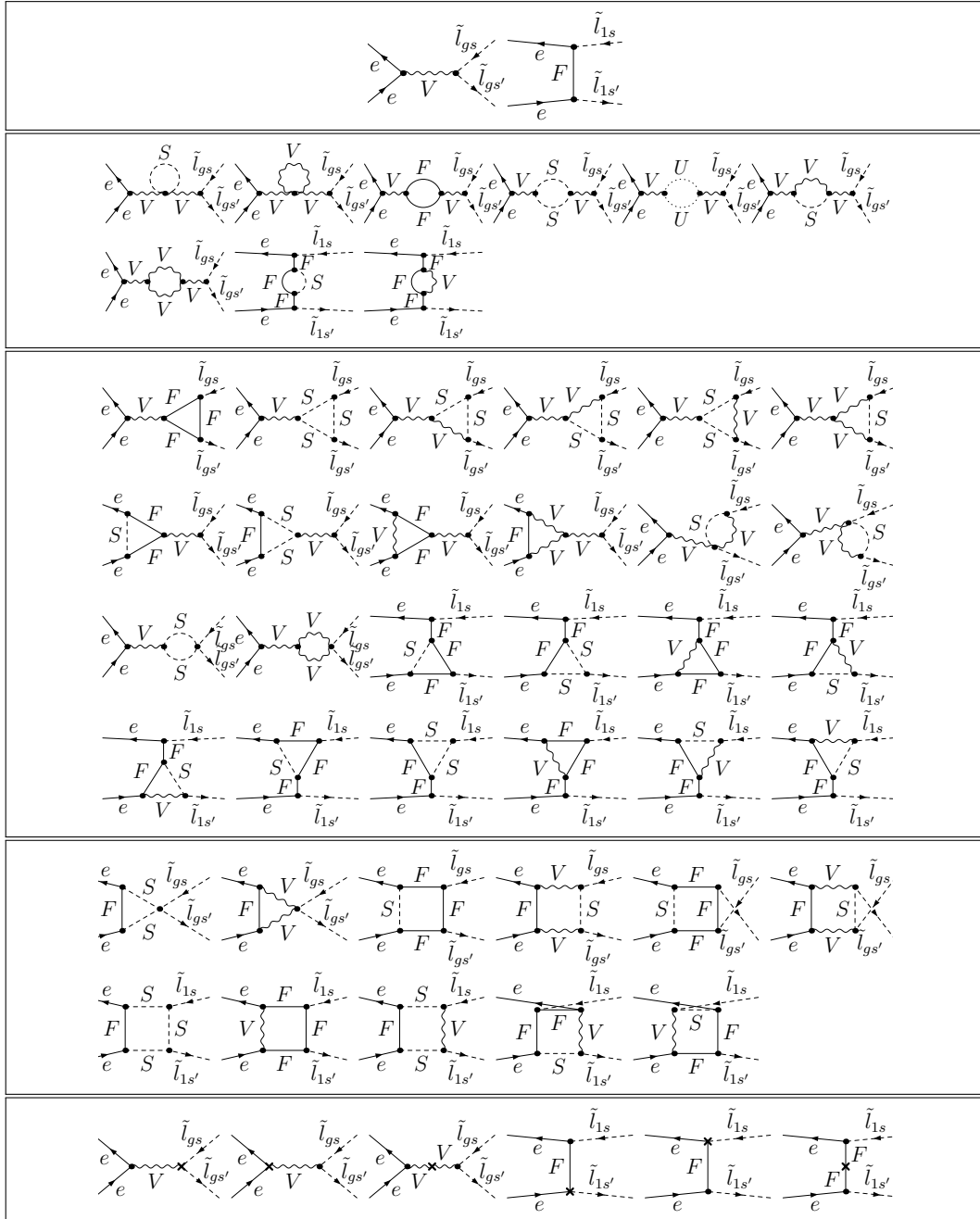


Figure 1: Generic tree, self-energy, vertex, box, and counterterm diagrams for the process $e^+e^- \rightarrow \tilde{l}_{gs}\tilde{l}_{gs'}$ ($\tilde{l}_{gs} = \{\tilde{e}_{gs}, \tilde{\nu}_g\}$; $g = 1, 2, 3$; $s, s' = 1, 2$). The additional diagrams, which occur only in the case of first generation slepton production, are denoted with \tilde{l}_{1s} . F can be a SM fermion, chargino or neutralino; S can be a sfermion or a Higgs/Goldstone boson; V can be a γ , Z or W^\pm . It should be noted that electron–Higgs couplings are neglected.

| Scen. | \sqrt{s} | t_β | μ | M_{H^\pm} | $M_{\tilde{Q},\tilde{U},\tilde{D}}$ | $M_{\tilde{L},\tilde{E}}$ | $ A_t $ | A_b | A_τ | $ M_1 $ | M_2 | M_3 |
|-------|------------|-----------|-------|-------------|-------------------------------------|---------------------------|---------|---------|-----------------|---------|---------|-------|
| S1 | 1000 | 10 | 450 | 500 | 1500 | 1500 | 2000 | $ A_t $ | $M_{\tilde{L}}$ | $\mu/4$ | $\mu/2$ | 2000 |

Table 1: MSSM default parameters for the numerical investigation of chargino and neutralino production; all parameters (except of t_β) are in GeV.

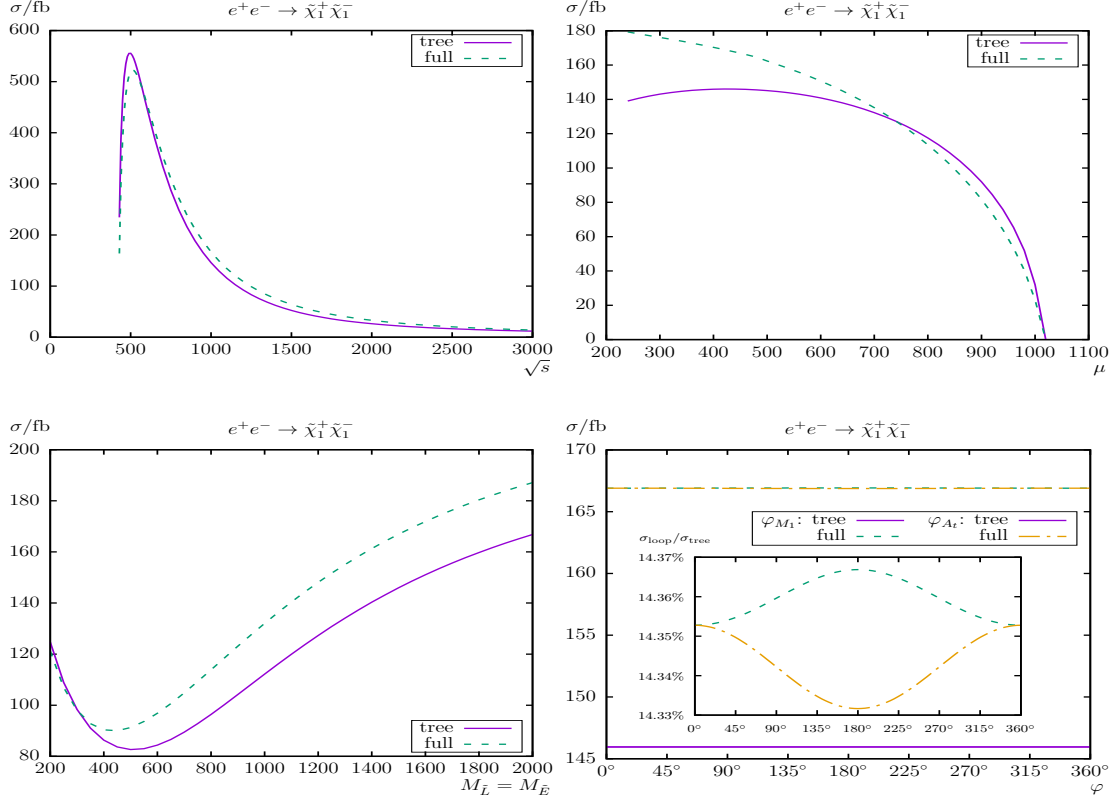


Figure 2: $\sigma(e^+e^- \rightarrow \tilde{\chi}_1^+ \tilde{\chi}_1^-)$. Tree-level and full one-loop corrected cross sections are shown with parameters chosen according to S1. The upper plots show the cross sections with \sqrt{s} (left) and μ (right) varied; the lower plots show $M_{\tilde{L}} = M_{\tilde{E}}$ (left) and $\varphi_{M_1}, \varphi_{A_i}$ (right) varied.

500 GeV and $\sim +14\%$ at $\sqrt{s} = 1000$ GeV are found in scenario S1, with a “tree crossing” (i.e. where the loop corrections become approximately zero and therefore cross the tree-level result) at $\sqrt{s} \approx 575$ GeV. The relative size of loop corrections increase with increasing \sqrt{s} (and decreasing σ) and reach $\sim +19\%$ at $\sqrt{s} = 3000$ GeV. With increasing μ in S1 (upper right plot) we find a strong decrease of the production cross section, as can be expected from kinematics. The relative loop corrections in S1 reach $\sim +30\%$ at $\mu = 240$ GeV (at the border of the experimental limit), $\sim +14\%$ at $\mu = 450$ GeV (i.e. S1) and $\sim -30\%$ at $\mu = 1000$ GeV. In the latter case these large loop corrections are due to the (relative) smallness of the tree-level results, which goes to zero for $\mu = 1020$ GeV (i.e. the chargino production threshold). The cross section as a function of $M_{\tilde{L}} (= M_{\tilde{E}})$ is shown in the lower left plot of Fig. 2. This mass parameter controls the t -channel exchange of first generation sleptons at tree-level. First a small decrease down to ~ 90 fb can be observed for $M_{\tilde{L}} \approx 400$ GeV. For larger $M_{\tilde{L}}$ the cross section rises up to ~ 190 fb for $M_{\tilde{L}} = 2$ TeV.

In scenario S1 we find a substantial increase of the cross sections from the loop corrections. They reach the maximum of $\sim +18\%$ at $M_{\tilde{L}} \approx 850$ GeV with a nearly constant offset of about 20 fb for higher values of $M_{\tilde{L}}$. We find that the phase dependence φ_{M_1} of the cross section in our scenario is tiny. The loop corrections are found to be nearly independent of φ_{M_1} at the level below $\sim +0.1\%$ in S1. We also show the variation with φ_{A_t} , which enter via final state vertex corrections. While the variation with φ_{A_t} is somewhat larger than with φ_{M_1} , it remains tiny and unobservable. However, in Ref. [14] other production channels with an appreciable phase dependence were identified.

3.2 The processes $e^+e^- \rightarrow \tilde{e}_{g_s}^\pm \tilde{e}_{g_s}^\mp$, and $e^+e^- \rightarrow \tilde{\nu}_g \tilde{\nu}_g^*$

The SUSY parameters for the numerical analysis for slepton production (i.e. in Ref. [15]) are chosen according to the scenario S2, shown in Tab. 2.

| Scen. | \sqrt{s} | t_β | μ | M_{H^\pm} | $M_{\tilde{Q},\tilde{U},\tilde{D}}$ | $M_{\tilde{E}}$ | A_{u_g} | A_{d_g} | $ A_{e_g} $ | $ M_1 $ | M_2 | M_3 |
|-------|------------|-----------|-------|-------------|-------------------------------------|-----------------|-----------|-----------|-------------|---------|-------|-------|
| S2 | 1000 | 10 | 350 | 1200 | 2000 | 300 | 2600 | 2000 | 2000 | 400 | 600 | 2000 |

Table 2: MSSM default parameters for the numerical investigation; all parameters (except of t_β) are in GeV. Furthermore, $M_{\tilde{L}} = M_{\tilde{E}} + 50$ GeV was chosen for all slepton generations.

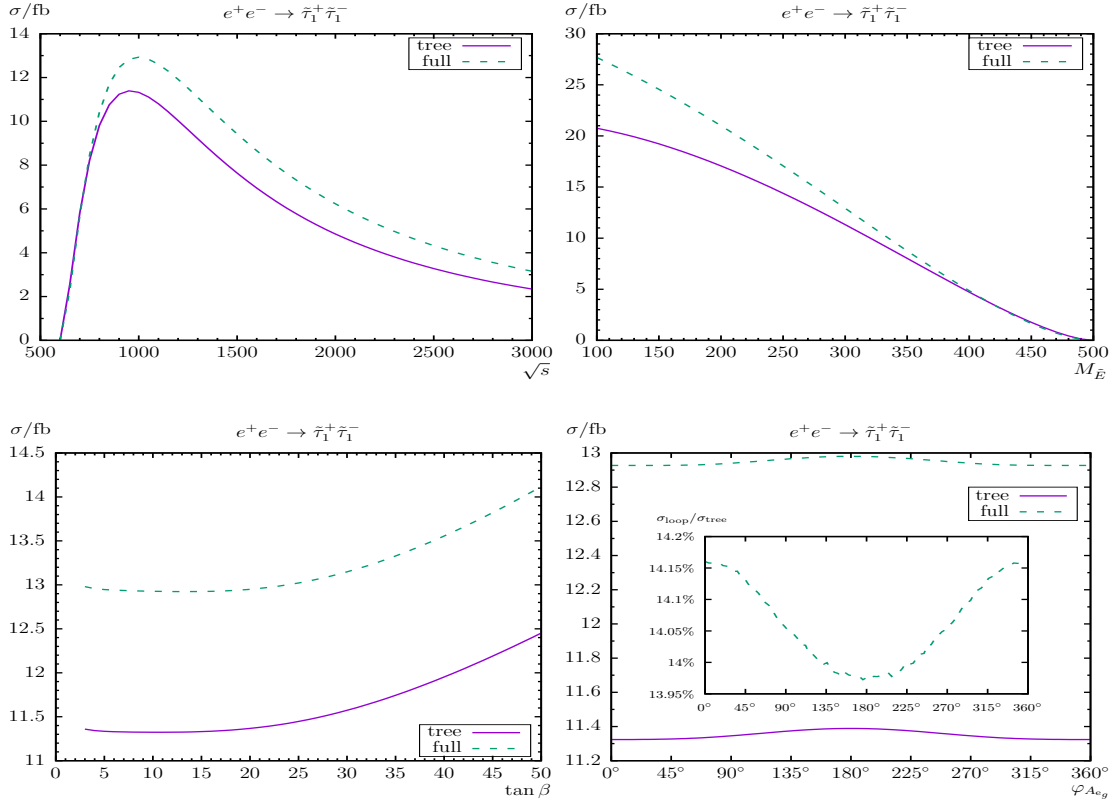


Figure 3: $\sigma(e^+e^- \rightarrow \tilde{\tau}_1^+ \tilde{\tau}_1^-)$. Tree-level and full one-loop corrected cross sections are shown with parameters chosen according to S2. The upper plots show the cross sections with \sqrt{s} (left) and $M_{\tilde{E}}$ (right) varied; the lower plots show t_β (left) and $\varphi_{A_{e_g}}$ (right) varied. All masses and energies are in GeV.

As an example of the numerical analysis presented in Ref. [15] we show the process $e^+e^- \rightarrow \tilde{\tau}_1^+ \tilde{\tau}_1^-$ in Fig. 3. As a function of \sqrt{s} we find loop corrections of $\sim +14\%$ at $\sqrt{s} = 1000$ GeV (i.e. S2), a tree crossing at $\sqrt{s} \approx 725$ GeV (where the one-loop corrections are between $\pm 10\%$ for $\sqrt{s} \lesssim 900$ GeV) and $\sim +35\%$ at $\sqrt{s} = 3000$ GeV. In the analysis as a function of $M_{\tilde{E}}$ (upper right plot) the cross sections are decreasing with increasing $M_{\tilde{E}}$ as obvious from kinematics and the full corrections have their maximum of ~ 28 fb at $M_{\tilde{E}} = 100$ GeV, more than two times larger than in S2. The relative corrections are changing from $\sim +33\%$ at $M_{\tilde{E}} = 100$ GeV to $\sim -25\%$ at $M_{\tilde{E}} = 490$ GeV with a tree crossing at $M_{\tilde{E}} = 415$ GeV. In the lower left row of Fig. 3 we show the dependence on t_β . The relative corrections for the t_β dependence vary between $\sim +14.2\%$ at $t_\beta = 5$ and $\sim +13.4\%$ at $t_\beta = 50$.

The phase dependence $\varphi_{A_{\text{eg}}}$ of the cross section in S2 is shown in the lower right plot of Fig. 3. The loop correction increases the tree-level result by $\sim +14\%$. The phase dependence of the relative loop correction is very small and found to be below 0.2% . The variation with φ_{M_1} is negligible and therefore not shown here.

Acknowledgements

S.H. thanks the organizers of L&L 2018 for the invitation and the (as always!) inspiring atmosphere. The work of S.H. is supported in part by the MEINCOP Spain under contract FPA2016-78022-P, in part by the ‘‘Spanish Agencia Estatal de Investigaci3n’’ (AEI) and the EU ‘‘Fondo Europeo de Desarrollo Regional’’ (FEDER) through the project FPA2016-78022-P, in part by the ‘‘Spanish Red Consolider MultiDark’’ FPA2017-90566-REDC, and in part by the AEI through the grant IFT Centro de Excelencia Severo Ochoa SEV-2016-0597.

References

- [1] H. Nilles, *Phys. Rept.* **110** (1984) 1; R. Barbieri, *Riv. Nuovo Cim.* **11** (1988) 1; H. Haber, G. Kane, *Phys. Rept.* **117** (1985) 75; J. Gunion, H. Haber, *Nucl. Phys.* **B 272** (1986) 1.
- [2] <https://twiki.cern.ch/twiki/bin/view/AtlasPublic/SupersymmetryPublicResults>.
- [3] <https://twiki.cern.ch/twiki/bin/view/CMSPublic/PhysicsResultsSUS>.
- [4] E. Bagnaschi et al., *Eur. Phys. J. C* **78** (2018) no.3, 256 [arXiv:1710.11091 [hep-ph]]; K. J. de Vries et al., *Eur. Phys. J. C* **75** (2015) no.9, 422 [arXiv:1504.03260 [hep-ph]].
- [5] S. Heinemeyer, arXiv:1801.05191 [hep-ph].
- [6] H. Baer et al., *The International Linear Collider Technical Design Report - Volume 2: Physics*, arXiv:1306.6352 [hep-ph]; R.-D. Heuer et al. [TESLA Collaboration], *TESLA Technical Design Report, Part III: Physics at an e^+e^- Linear Collider*, arXiv:hep-ph/0106315, see: http://tesla.desy.de/new_pages/TDR_CD/start.html; K. Ackermann et al., *Proceedings Summer Colloquium, Amsterdam, Netherlands, 4 April 2003*, DESY-PROC-2004-01; J. Brau et al. [ILC Collaboration], *ILC Reference Design Report Volume 1 - Executive Summary*, arXiv:0712.1950 [physics.acc-ph]; A. Djouadi et al. [ILC Collaboration], *International Linear Collider Reference Design Report Volume 2: Physics at the ILC*, arXiv:0709.1893 [hep-ph].
- [7] G. Moortgat-Pick et al., *Eur. Phys. J. C* **75** (2015) 8, 371 [arXiv:1504.01726 [hep-ph]].

- [8] L. Linssen, A. Miyamoto, M. Stanitzki, H. Weerts, [arXiv:1202.5940](#) [physics.ins-det]; H. Abramowicz et al. [CLIC Detector and Physics Study Collaboration], *Physics at the CLIC e^+e^- Linear Collider – Input to the Snowmass process 2013*, [arXiv:1307.5288](#) [hep-ex].
- [9] G. Weiglein et al. [LHC/ILC Study Group], *Phys. Rept.* **426** (2006) 47 [[arXiv:hep-ph/0410364](#)]; A. De Roeck et al., *Eur. Phys. J. C* **66** (2010) 525 [[arXiv:0909.3240](#) [hep-ph]]; A. De Roeck, J. Ellis, S. Heinemeyer, *CERN Cour.* **49N10** (2009) 27.
- [10] S. Heinemeyer, C. Schappacher, *Eur. Phys. J. C* **72** (2012) 2136 [[arXiv:1204.4001](#) [hep-ph]].
- [11] S. Heinemeyer, F. von der Pahlen, C. Schappacher, *Eur. Phys. J. C* **72** (2012) 1892 [[arXiv:1112.0760](#) [hep-ph]]; A. Bharucha, S. Heinemeyer, F. von der Pahlen, C. Schappacher, *Phys. Rev.* **D 86** (2012) 075023 [[arXiv:1208.4106](#) [hep-ph]]; A. Bharucha, S. Heinemeyer, F. von der Pahlen, *Eur. Phys. J. C* **73** (2013) 2629 [[arXiv:1307.4237](#) [hep-ph]].
- [12] S. Heinemeyer, C. Schappacher, *Eur. Phys. J. C* **75** (2015) 5, 198 [[arXiv:1410.2787](#) [hep-ph]].
- [13] S. Heinemeyer, C. Schappacher, *Eur. Phys. J. C* **75** (2015) 5, 230 [[arXiv:1503.02996](#) [hep-ph]].
- [14] S. Heinemeyer, C. Schappacher, *Eur. Phys. J. C* **77** (2017) 9, 649 [[arXiv:1704.07627](#) [hep-ph]].
- [15] S. Heinemeyer, C. Schappacher, *Eur. Phys. J. C* **178** (2018) 7, 536 [[arXiv:1803.10645](#) [hep-ph]].
- [16] S. Heinemeyer and C. Schappacher, [arXiv:1801.05192](#) [hep-ph].
- [17] J. Küblbeck, M. Böhm, A. Denner, *Comput. Phys. Commun.* **60** (1990) 165; T. Hahn, *Comput. Phys. Commun.* **140** (2001) 418 [[arXiv:hep-ph/0012260](#)]; T. Hahn, C. Schappacher, *Comput. Phys. Commun.* **143** (2002) 54 [[arXiv:hep-ph/0105349](#)].
Program, user's guide and model files are available via: <http://www.feynarts.de>.
- [18] T. Fritzsche, T. Hahn, S. Heinemeyer, F. von der Pahlen, H. Rzehak, C. Schappacher, *Comput. Phys. Commun.* **185** (2014) 1529 [[arXiv:1309.1692](#) [hep-ph]].
- [19] T. Hahn, M. Pérez-Victoria, *Comput. Phys. Commun.* **118** (1999) 153 [[arXiv:hep-ph/9807565](#)].
Program and user's guide are available via: <http://www.feynarts.de/formcalc/>; T. Hahn, S. Paßehr, C. Schappacher, *PoS LL2016 (2016) 068*, *J. Phys. Conf. Ser.* **762** (2016) 1, 012065 [[arXiv:1604.04611](#) [hep-ph]].
- [20] M. Frank, T. Hahn, S. Heinemeyer, W. Hollik, H. Rzehak, G. Weiglein, *JHEP* **0702** (2007) 047 [[arXiv:hep-ph/0611326](#)].
- [21] S. Heinemeyer, H. Rzehak, C. Schappacher, *Phys. Rev.* **D 82** (2010) 075010 [[arXiv:1007.0689](#) [hep-ph]].
- [22] T. Fritzsche, S. Heinemeyer, H. Rzehak, C. Schappacher, *Phys. Rev.* **D 86** (2012) 035014 [[arXiv:1111.7289](#) [hep-ph]].
- [23] S. Heinemeyer, C. Schappacher, *Eur. Phys. J. C* **72** (2012) 1905 [[arXiv:1112.2830](#) [hep-ph]].
- [24] S. Heinemeyer, C. Schappacher, *Eur. Phys. J. C* **76** (2016) 4, 220 [[arXiv:1511.06002](#) [hep-ph]].
- [25] S. Heinemeyer, C. Schappacher, *Eur. Phys. J. C* **76** (2016) 10, 535 [[arXiv:1606.06981](#) [hep-ph]].
- [26] F. del Aguila, A. Culatti, R. Muñoz-Tapia, M. Pérez-Victoria, *Nucl. Phys.* **B 537** (1999) 561 [[arXiv:hep-ph/9806451](#)].
- [27] W. Siegel, *Phys. Lett.* **B 84** (1979) 193.
- [28] D. Capper, D. Jones, P. van Nieuwenhuizen, *Nucl. Phys.* **B 167** (1980) 479.
- [29] D. Stöckinger, *JHEP* **0503** (2005) 076 [[arXiv:hep-ph/0503129](#)].
- [30] W. Hollik, D. Stöckinger, *Phys. Lett.* **B 634** (2006) 63 [[arXiv:hep-ph/0509298](#)].